

Open Research Online

The Open University's repository of research publications and other research outputs

ISO-LWS grating spectroscopy: the case of R CrA star forming region

Conference or Workshop Item

How to cite:

Giannini, T.; Lorenzotti, D.; Benedettini, M.; Nisini, B.; Saraceno, P.; Tommasi, E.; Smith, H. A. and White, G. J. (1998). ISO-LWS grating spectroscopy: the case of R CrA star forming region. In: Star Formation with the Infrared Space Observatory, 24-26 Jun 1997, Lisbon, Portugal.

For guidance on citations see [FAQs](#).

© 1998 Astronomical Society of the Pacific

Version: Version of Record

Link(s) to article on publisher's website:
<http://www.aspbbooks.org/publications/132/350.pdf>

Copyright and Moral Rights for the articles on this site are retained by the individual authors and/or other copyright owners. For more information on Open Research Online's data [policy](#) on reuse of materials please consult the policies page.

oro.open.ac.uk

ISO-LWS Grating Spectroscopy: The Case of R CrA Star Forming Region

T. Giannini, D. Lorenzetti, M. Benedettini, B. Nisini, P. Saraceno
IFSI - CNR, Frascati, Italy

E. Tommasi
ISO Science Operation Centre - Villafranca, Madrid (Spain)

H.A. Smith
Harvard-Smithsonian Center for Astrophysics - Cambridge (USA)

G.J. White
Queen Mary & Westfield College - London (UK)

Abstract. We present the far infrared spectra of the R CrA star forming region obtained with ISO-LWS. We collected a pointed observation on the Herbig Ae star R CrA and a raster scan covering the surrounding region, where HH100 (with its exciting source) and the pre-Main Sequence star T CrA are located. The [OI] $63\mu\text{m}$ and the [CII] $158\mu\text{m}$ lines have been detected in all the pointed positions, with a ratio consistent with PDR excitation. CO rotational lines (between $J_{up}=14$ and $J_{up}=19$) are detected on R CrA; from their intensities we derived, using a LVG model, the density and temperature of the emitting region. Other molecular transitions (OH and H₂O) have been detected on the investigated objects; the derived cooling of all the molecular species is in agreement with C-shock as the likely excitation mechanism. The continuum emission of R CrA peaks around $100\mu\text{m}$ (as expected for a Herbig star) while the other sources (T CrA, HH100) show increasing continua up to $\sim 200\mu\text{m}$, indicating that they are probably less evolved sources.

1. The R CrA region

The Corona Australis (CrA) molecular cloud is an active center of intermediate and low mass star formation (Graham 1991), located at high galactic latitude ($l=0^\circ$, $b=-18^\circ$) at a distance of ~ 150 pc. It contains several pre-Main Sequence stars (S CrA, T CrA, TY CrA, VV CrA), some presumably less evolved objects (IRS 7, HH100IR) and manifestations of mass ejection (HH 98, HH99, HH100, HHs101, HHs104). The ¹²CO map ($J=2\rightarrow 1$) (Levreault 1988) revealed a complex structure explained with a superposition of two separate bipolar outflows: a strong compact one, E-W oriented, centered on the deeply embedded source

IRS 7 (Anderson et al. 1997), and a more extended one centered on the source HH100-IR (Strom et al. 1974).

2. Observations and Results

We observed the R CrA region with the LWS set in grating mode (wavelength range 43 - 196.7 μm , $R \sim 200$, $\text{FOV} \sim 80''$, oversampling of 4 of the resolution element). We pointed R CrA itself and made a 3×1 raster map covering T CrA, HH100 and an *off* position.

Table 1. Observed line intensities

λ (obs.) (μm)	Line ident.	R CrA	T CrA	HH100	off
		$F \pm \Delta F^\dagger$ ($10^{-19} \text{ W cm}^{-2}$)			
63.2	[OI] $^3P_2 \rightarrow ^3P_1$	58 ± 1	19 ± 1	9.4 ± 0.4	2.1 ± 0.3
71.2	OH $^2\Pi_{1/2, J=7/2} \rightarrow ^2\Pi_{1/2, J=5/2}$	<2.4	1.7 ± 0.5	-	-
79.2	OH $^2\Pi_{1/2, J=1/2} \rightarrow ^2\Pi_{3/2, J=3/2}$	4 ± 1	-	<1.1	-
84.6	OH $^2\Pi_{3/2, J=7/2} \rightarrow ^2\Pi_{3/2, J=5/2}$	9 ± 2	-	<1.3	-
99.5	$\text{o-H}_2\text{O } 5_{05} \rightarrow 4_{14}$	-	1.8 ± 0.5	-	-
137.2	CO $19 \rightarrow 18$	4 ± 1	-	-	-
144.8	CO $18 \rightarrow 17$	$<6.8^*$	-	-	-
145.5	[OI] $^3P_1 \rightarrow ^3P_0$	$<4.3^*$	2.4 ± 0.7	<1.6	0.3 ± 0.1
153.2	CO $17 \rightarrow 16$	5.8 ± 0.9	4 ± 1	1.8 ± 0.6	<0.3
157.7	[CII] $^2P_{1/2} \rightarrow ^2P_{3/2}$	3 ± 1	4 ± 1	2.3 ± 0.9	0.7 ± 0.1
162.8	CO $16 \rightarrow 15$	6.4 ± 0.9	<2.3	$2.5 \pm 0.5^*$	0.39 ± 0.07
163.4	OH $^2\Pi_{1/2, J=3/2} \rightarrow ^2\Pi_{1/2, J=1/2}$	-	-	$2.0 \pm 0.5^*$	-
173.7	CO $15 \rightarrow 14$	5.8 ± 0.6	2.5 ± 0.6	1.9 ± 0.3	-
174.7	$\text{o-H}_2\text{O } 3_{03} - 2_{12}$	-	-	<1.2	-
179.6	$\text{o-H}_2\text{O } 2_{12} - 1_{01}$	-	2.1 ± 0.4	-	-
186.0	CO $14 \rightarrow 13$	4.6 ± 0.6	<1.2	-	-

Notes: † 1σ statistical error, * lines de-blended with a two gaussian fit.

The identified transitions and the corresponding integrated intensities are listed in Table 1. The [OI] and [CII] lines are detected in all the pointed positions, while the molecular emission is dominated by the CO rotational lines along with the OH and H₂O transitions.

3. Line Diagnostics

In Figure 1a the observed line intensities ratios of $[\text{OI}]63\mu\text{m}/[\text{OI}]145\mu\text{m}$ vs. $[\text{OI}]63\mu\text{m}/[\text{CII}]158\mu\text{m}$ are superposed to PDR emission models for different values of density and interstellar fields strengths (Luhman M., private communication). The line intensities result from ON-OFF subtraction and their ratios indicate that the emission is consistent with a PDR mechanism; R CrA is associated with a density higher than the other objects in the region. PDR emission is also supported by comparing \dot{M}_{CO} , derived from the literature, with $\dot{M}_{[\text{OI}]}$, *i.e.* the mass loss derived assuming that all the OI emission is shock excited (Hollenbach 1985) (Table 2). In all objects $\dot{M}_{[\text{OI}]}$ is systematically larger than \dot{M}_{CO} , indicating a probable excess of [OI] emission due to PDR.

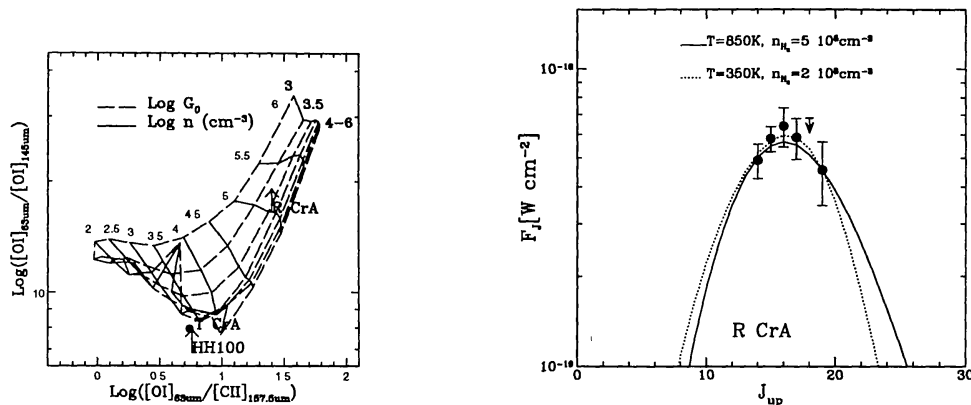


Figure 1. a) Observed line ratios superposed to PDR models. The arrows indicate 3σ upper limits. b) CO line fluxes observed by LWS in R CrA *vs.* J_{up} . The lines give the possible fits through the data.

We have modelled the CO lines observed in the R CrA by using a large velocity gradient (LVG) code in the plane-parallel geometry (Nisini et al. this issue). Figure 1b shows the CO fluxes as a function of the rotational quantum number J_{up} . The dashed and solid lines give the range of the possible model fits to the data and the relative parameters are indicated. Although we observe only few CO transitions, they seem to trace the peak of the distribution, allowing a stringent constraint to the parameters. The possible ranges of temperature and density are $T=350 \div 850$ K and $n_{H_2} = 2 \times 10^6 \div 5 \times 10^5$ cm^{-3} . For the low temperature model we derived a CO column density of 6×10^{18} cm^{-2} and an emitting region of $5 \div 6$ arcsec.

To recognize the mechanism responsible for the molecular emission we plot in Figure 2a the luminosity ratio of OI/CO and CO/OH as a function of the density for different shock velocities, according to the model of Draine et al. (1983). Both ratios indicate that the C-shock is likely the mechanism for molecular line excitation. The ratio $L(\text{OI})/L(\text{CO})$ (top panel) is overestimated because of a possible contribution from PDR emission, not taken in account in the model. In the case of R CrA the indication of a post-shock density $n_{post-shock} \sim 10^6$ cm^{-3} (by the CO LVG model) allows to derive a shock velocity $20 \div 40$ Km s^{-1} , assuming a shock compression factor $n_{post-shock}/n_{pre-shock} \sim 10-100$.

Table 2. **Derived PDR Parameters**

Source	Density (cm^{-3})	Field (G_\odot)	\dot{M} ([OI] 63 μm) ($M_\odot \text{yr}^{-1}$)	\dot{M} (CO) ($M_\odot \text{yr}^{-1}$)
R CrA	$>10^5$	$<10^4$	$3.8 \cdot 10^{-6}$	$3.8 \cdot 10^{-7}$
T CrA	$3 \cdot 10^3 \div 10^4$	$\sim 10^4$	$1.2 \cdot 10^{-6}$	$3.8 \cdot 10^{-7}$
HH 100	$>3 \cdot 10^3$	$<10^4$	$5.0 \cdot 10^{-7}$	$1.4 \cdot 10^{-7}$

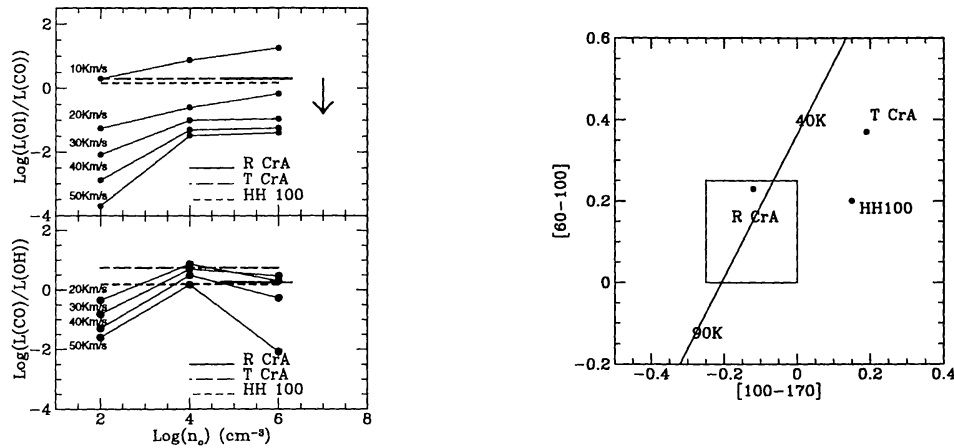


Figure 2. a) Luminosity ratios of OI/CO and CO/OH compared with C-shock models. b) ISO two colours diagram.

4. The continuum data

In Table 3 the flux densities of R CrA, T CrA and HH100 at 60, 100 and 170 μm (and the relative colours) are reported. As expected for a Herbig star, the continuum of R CrA peaks around 100 μm , while the other objects peak at longer wavelengths, thus revealing an earlier stage of evolution.

Table 3. FIR flux densities and ISO colours

Source	Flux (60 μm)	Flux (100 μm) (Jy)	Flux (170 μm)	[60-100]	[100-170]
R CrA	729	1227	937	0.23	-0.12
T CrA	190	300	427	0.20	0.19
HH 100	151	353	546	0.37	0.15

In Figure 2b an ISO two colours diagram is given. The temperatures of different blackbodies (BBs) are reported as a solid line, while the square indicates the locus of the Herbig stars (Tommasi et al., this issue). We note that the R CrA colours are consistent with an envelope of $T \sim 50\text{K}$, while the other observed colours are not fitted with a single BB, but at least two thermal components are required.

References

- Anderson I.M., Harju J., Knee L.B.G., Haikala L.K. 1997, A&A, 321, 575
 Draine B.T., Roberge W.G., Dalgarno A. 1983, ApJ, 264, 485
 Graham J.A. 1991, ESO Report N.11, Reipurth B. (ed.), pp 185-196
 Hollenbach D.J. 1985, Icarus, 61, 36
 Levreault R.M. 1988, ApJS, 67, 283
 Strom K.M., Strom S.E., Grasdalen G.L. 1974, ApJ, 187, 83